The Astrophysical Journal Letters, 912:L20 (6pp), 2021 May 10 https://doi.org/10.3847/2041-8213/abf9a5

Resolving the Complex Evolution of a Supermassive Black Hole Triplet in a Cosmological Simulation

Matias Mannerkoski[1], Peter H. Johansson[1], Antti Rantala[2], Thorsten Naab[2], and Shihong Liao[1]
[1] Department of Physics, Gustaf Hällströmin katu 2, FI-00014, University of Helsinki, Finland; matias.mannerkoski@helsinki.fi
[2] Max-Planck-Institut für Astrophysik, Karl-Schwarzchild-Str 1, D-85748 Garching, Germany
Received 2021 March 30; revised 2021 April 19; accepted 2021 April 20; published 2021 May 6

Abstract

We present here a self-consistent cosmological zoom-in simulation of a triple supermassive black hole (SMBH) system forming in a complex multiple galaxy merger. The simulation is run with an updated version of our code KETJU, which is able to follow the motion of SMBHs down to separations of tens of Schwarzschild radii while simultaneously modeling the large-scale astrophysical processes in the surrounding galaxies, such as gas cooling, star formation, and stellar and AGN feedback. Our simulation produces initially an SMBH binary system for which the hardening process is interrupted by the late arrival of a third SMBH. The KETJU code is able to accurately model the complex behavior occurring in such a triple SMBH system, including the ejection of one SMBH to a kiloparsec-scale orbit in the galaxy due to strong three-body interactions as well as Lidov–Kozai oscillations suppressed by relativistic precession when the SMBHs are in a hierarchical configuration. One pair of SMBHs merges ∼3 Gyr after the initial galaxy merger, while the remaining binary is at a parsec-scale separation when the simulation ends at redshift $z = 0$. We also show that KETJU can capture the effects of the SMBH binaries and triplets on the surrounding stellar population, which can affect the binary merger timescales as the stellar density in the system evolves. Our results demonstrate the importance of dynamically resolving the complex behavior of multiple SMBHs in galactic mergers, as such systems cannot be readily modeled using simple orbit-averaged semianalytic models.

Unified Astronomy Thesaurus concepts: Supermassive black holes (1663); Galaxy mergers (608); Astronomical simulations (1857)

1. Introduction

Supermassive black holes (SMBHs) with masses in the range of $M_{\rm BH} = 10^6$–$10^{10} M_\odot$ are found in the centers of all massive galaxies (Kormendy & Ho 2013). In the ΛCDM hierarchical model galaxies grow through mergers and gas accretion, with the coalescence of SMBHs in galactic mergers proceeding through three stages (Begelman et al. 1980). First, the separation between the SMBHs shrinks from the initial kiloparsec scale due to dynamical friction (Chandrasekhar 1943) from the surrounding stars and gas in the galaxy until the SMBHs form a bound binary with a typical separation of $a \sim 1$–10 pc. From there the binary will further shrink ("harden") due to scattering of individual stars that carry away energy and angular momentum (Hills & Fullerton 1980). Finally, at subparsec scales gravitational-wave (GW) emission becomes the dominant mechanism for energy loss and drives the SMBH binary to coalescence (Peters & Mathews 1963; Peters 1964).

Given a suitable galactic environment where the lifetime of the SMBH binary exceeds the time between galactic mergers, systems that include multiple interacting SMBHs may form (e.g., Hoffman & Loeb 2007). The triplet is the simplest multiple SMBH configuration, and the dynamics of such systems have been extensively studied in isolated simulations, including a semianalytic treatment of the stellar environment (Hoffman & Loeb 2007; Bonetti et al. 2016, 2019). In addition, there is now increasingly strong evidence that such systems are relatively commonplace, as several triplet SMBHs have been observed in the local universe (Deane et al. 2014; Liu et al. 2019; Pfeifle et al. 2019; Kollatschny et al. 2020).

Modeling the entire SMBH coalescence process beyond the formation of a bound binary has not previously been possible in a full cosmological simulation due to the inability of simultaneously modeling the small-scale dynamics and global galactic-scale processes in simulations that include gravitational force softening (Kelley et al. 2017a; Ryu et al. 2018). Some improvements on the SMBH behavior at kiloparsec scales have been achieved with the addition of subgrid models of the unresolved dynamical friction contribution (Tremmel et al. 2015; Pfister et al. 2019). However, the parsec-scale dynamics has in general been modeled by postprocessing the simulations using semianalytic methods based on orbit-averaged equations (Kelley et al. 2017a, 2017b) or by resimulating the core regions of the merged galaxies using an altogether separate *N*-body code (Khan et al. 2016). Both of these approaches break the coupling of the small-scale SMBH dynamics with the global simulation, which affects the ability to self-consistently model the evolution of the stellar structure of the galaxy and may have important consequences for both the merger timescales of the SMBHs and the structure of the final galaxy (Rantala et al. 2018).

In this Letter we present a self-consistent cosmological zoom-in simulation of a triple SMBH system forming in a complex multiple galaxy merger at redshift $z \sim 0.5$. The simulation is run with our KETJU code, which is capable of following the motion of SMBHs down to separations of tens of Schwarzschild radii while simultaneously modeling the large-scale processes in the surrounding galaxies.

2. Numerical Simulations

2.1. The KETJU Code

The simulations are run using the KETJU code (Rantala et al. 2017), which is an extension of the widely used GADGET-3 code

(Springel 2005). In the KETJU code the dynamics of SMBHs and the stars in a small region around them are integrated with an algorithmically regularized integrator, whereas the dynamics of the remaining particles is computed with the GADGET-3 leapfrog using the tree-PM force calculation method. The application of an algorithmically regularized integrator enables the accurate modeling of dynamical friction on SMBHs and SMBH binary hardening, provided that the SMBH mass to stellar particle mass ratio is large enough. A mass ratio of ∼500–1000 has been observed to give converged results with only a weak resolution dependence (Rantala et al. 2017).

In this Letter we have replaced the regularized AR-CHAIN (Mikkola & Merritt 2008) integrator used in the first KETJU version (Rantala et al. 2017) with the new MSTAR integrator (Rantala et al. 2020), which has a significantly improved parallelization scheme and an improved interface with the main GADGET-3 code. Together these improvements allow for simulations containing up to $\sim 10^4$ particles in the regularized regions without the computational cost becoming prohibitive, which is a significant improvement on the previous KETJU studies (Rantala et al. 2017, 2018, 2019; Mannerkoski et al. 2019).

The integration within each regularized region is performed in physical center-of-mass coordinates, converted from (to) the comoving coordinates used in the main integrator at the start (end) of each integration, while the center of mass of the system is propagated in comoving coordinates. This correctly captures the motion of the system in an expanding universe. We set the relative per step error tolerance of the integrator to $\eta = 10^{-8}$ in order to ensure accurate evolution also in the GW-dominated regime. To model the effects of general relativity on the motion of the SMBHs, KETJU includes post-Newtonian (PN) correction terms up to order 3.5 between each pair of SMBHs (Mora & Will 2004). However, mergers of SMBHs are currently implemented in KETJU only in a simplified fashion conserving the Newtonian linear and angular momentum as well as the total mass of the system, with the SMBHs being merged at a separation of six Schwarzschild radii.

Finally, in order to avoid possible energy errors caused by interactions between stellar particles just within and outside the rather large regularized regions, we now also employ gravitational softening for the stellar particle interactions inside the regularized regions. The introduction of stellar softening does not negatively affect the accuracy of the SMBH dynamics as all interactions involving SMBHs are still nonsoftened.

2.2. Hydrodynamics and Feedback

Contrary to our earlier KETJU studies, the simulations presented here also include a gas component and both stellar and BH feedback. The hydrodynamics are modeled using the modern SPHGal smoothed particle hydrodynamics (SPH) implementation (Hu et al. 2014), which employs a pressure-entropy formulation together with artificial conduction, artificial viscosity, and a Wendland C^4-kernel smoothed over 100 neighbors. Currently, the small-scale gas dynamics around the SMBHs is not resolved below the softening scale of the simulation.

For stellar physics and gas cooling we use metal-dependent cooling models tracking 11 individual elements (Scannapieco et al. 2005, 2006; Aumer et al. 2013). Our star formation model stochastically converts gas particles to stellar particles based on the local star formation timescale above a critical hydrogen number density of $n_{\rm H} = 0.1\ {\rm cm}^{-3}$. Other features of the models include feedback on gas from supernovae and massive stars and the production of metals through stellar chemical evolution (Aumer et al. 2013; Eisenreich et al. 2017).

Galaxies with dark matter halo masses of $M_{\rm DM} = 10^{10} h^{-1} M_\odot$ are seeded with SMBHs with masses of $M_\bullet = 10^5 h^{-1} M_\odot$ (Sijacki et al. 2007). Black holes grow through accretion and merging, with the accretion modeled using a standard Bondi–Hoyle–Lyttleton prescription with an additional dimensionless multiplier $\alpha = 25$ to account for the limited spatial resolution (Johansson et al. 2009a). The accretion rate is capped at the Eddington limit assuming a radiative efficiency of $\epsilon_r = 0.1$ and with 5% of the radiated energy coupling to the surrounding gas as thermal energy (Springel et al. 2005). A drawback of this accretion model is that it does not properly model accretion onto SMBHs in a binary system. However, this shortcoming is not significant for the particular binary and triple SMBH systems that we are concentrating on in this study, as the gas surrounding the black holes during the binary phase is very dilute and hence the corresponding accretion rates are very low.

Due to the mass ratio requirement we only switch on the regularized dynamics after the SMBHs of interest have grown to sufficiently large masses. Before the regularized dynamics are switched on, i.e., when using standard GADGET-3, the SMBHs are kept in the centers of their host galaxies using a simple repositioning method (Johansson et al. 2009b), which allows them to grow to realistic masses due to merging and gas accretion.

2.3. Initial Conditions and Simulations

We perform a cosmological zoom-in simulation starting at a redshift of $z = 50$ centered on a massive dark matter halo with a virial mass of $M_{200} \sim 7.5 \times 10^{12} M_\odot$ at $z = 0$. The initial conditions for our simulation are generated with the MUSIC (Hahn & Abel 2011) software package. We use the Planck 2018 cosmology (Planck Collaboration et al. 2020): $\Omega_m = 0.315$, $\Omega_b = 0.0491$, $\Omega_\Lambda = 0.685$, $H_0 = h \times 100\ {\rm km\ s^{-1}\ Mpc^{-1}} = 67.4\ {\rm km\ s^{-1}\ Mpc^{-1}}$, $\sigma_8 = 0.81$, and $n_s = 0.965$.

The target halo is selected from an initial run of a uniform dark matter only box with a comoving side length of $100 h^{-1}$ Mpc and 256^3 particles. We then generate new initial conditions with four levels of refinement around the Lagrangian volume of the target halo, so that the highest-resolution region contains approximately a total of $\sim 2 \times 200^3$ particles, with an equal number of gas and dark matter particles. This results in a dark matter particle mass of $m_{\rm DM} = 1.6 \times 10^6 M_\odot$ and a gas particle mass of $m_{\rm gas} = 3 \times 10^5 M_\odot$ in the high-resolution region.

The gravitational softening lengths are initially fixed in comoving coordinates. Below redshift $z = 9$ the softening lengths are fixed in physical coordinates at values of $\epsilon_{\rm bar} = 40 h^{-1}$ pc for stars and gas and $\epsilon_{\rm DM,high} = 93 h^{-1}$ pc for high-resolution dark matter particles. The low resolution boundary dark matter particles have correspondingly much larger softening lengths of $\epsilon_{\rm DM,low} = 5.96 h^{-1}$ kpc. The radii of the regularized regions were set to $120 h^{-1}$ pc, corresponding to $3 \times \epsilon_{\rm bar}$.

3. Results

3.1. Simulation Overview

We initially run the simulation with standard GADGET-3 without the KETJU SMBH dynamics enabled. At redshift $z \approx 0.62$ the target halo hosts three massive galaxies (A, B and

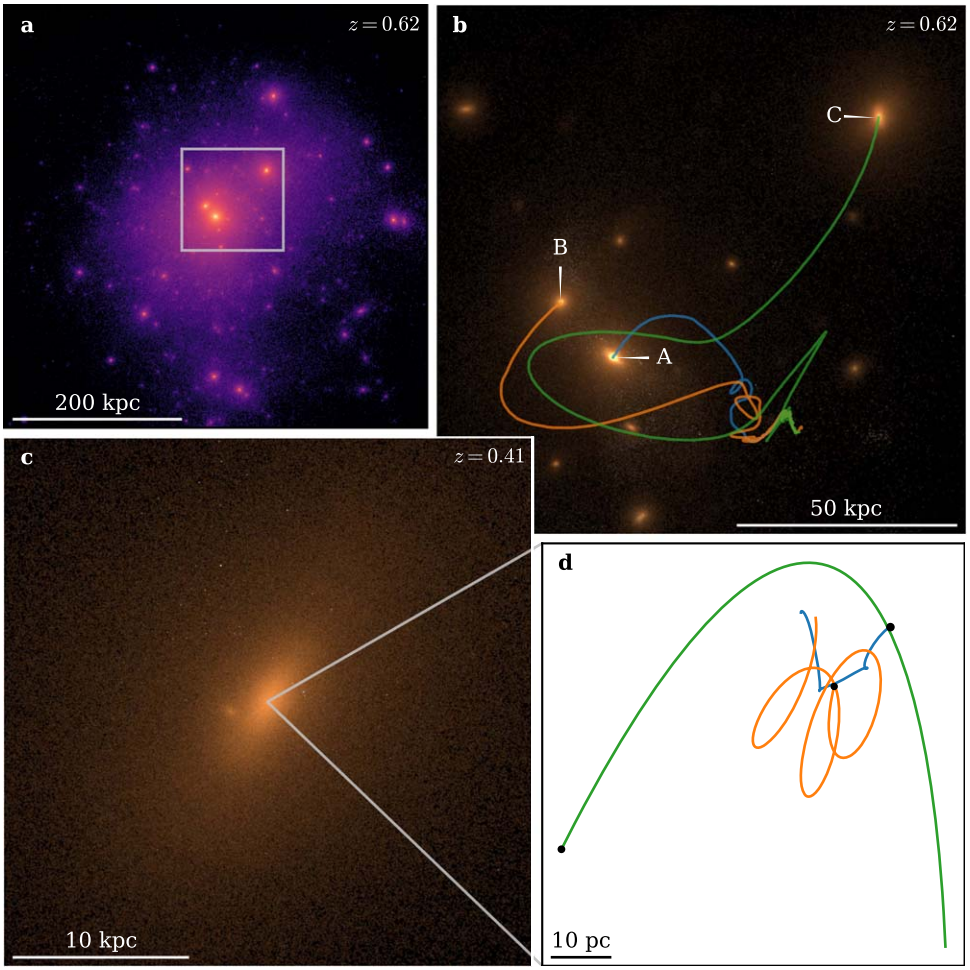

Figure 1. Overview of the simulation, showing the different physical scales modeled. (a) The simulated dark matter halo, showing the projected mass density at redshift $z \approx 0.62$ corresponding to cosmic time $t \approx 7.8$ Gyr when the KETJU dynamics were switched on. The box marks the region shown in panel (b). (b) A BVR image of the main galaxies A, B, and C, with the colored lines showing the subsequent trajectories of their central SMBHs until $z = 0$. (c) The galaxy formed after galaxies A, B, and C have merged shown at $z \approx 0.41$ ($t \approx 9.3$ Gyr). (d) The three SMBHs interacting in the center of the galaxy, showing sections of their trajectories spanning 1 Myr.

C; Figure 1(b)) with stellar masses of $M_{*,A} = 1.4 \times 10^{11} M_\odot$, $M_{*,B} = 5.4 \times 10^{10} M_\odot$, and $M_{*,C} = 6.3 \times 10^{10} M_\odot$ (within 30 kpc; all distances in this section are measured in physical coordinates). These galaxies host massive central SMBHs with masses of $M_{\bullet,A} = 8.4 \times 10^8 M_\odot$, $M_{\bullet,B} = 1.1 \times 10^8 M_\odot$, and $M_{\bullet,C} = 2.1 \times 10^8 M_\odot$, which are consistent with observed galaxies of similar masses (Kormendy & Ho 2013). At this stage the mass ratio between these SMBHs and the stellar particles (mean $m_{\rm part} \approx 2.5 \times 10^5 M_\odot$) is sufficiently large to allow for detailed dynamical modeling using KETJU. The corresponding gas fractions within 1 kpc from these SMBHs are very low at $f_{\rm gas} = M_{\rm gas}/(M_{\rm gas} + M_*) \sim 10^{-4}$. From this point on, we continued the simulation using two different configurations, with one simulation run using KETJU and the other run continued with standard GADGET-3 without SMBH repositioning to demonstrate the effects of our improved SMBH dynamics compared to softened dynamics. Both simulations were run until redshift $z = 0$.

3.2. Galaxy Mergers and SMBH Orbital Evolution

Galaxy B merges with galaxy A at a redshift of $z \approx 0.48$. In the KETJU simulation the SMBH of galaxy B sinks to the center of the merger remnant and forms a binary with SMBH-A (AB-binary) with a semimajor axis of $a_{\rm AB} \approx 100$ pc. Over the following ~250 Myr stellar scattering hardens the binary to a semimajor axis of $a_{\rm AB} \approx 10$ pc (Figure 2). During this time period, galaxy C merges with the system as well, which results in a three-body interaction between the three SMBHs as SMBH-C sinks to the center of the system. Initially this interaction causes rapid changes in the eccentricity of the AB-binary, and finally SMBH-B is ejected from the center with SMBH-C taking its place in a new binary with SMBH-A.

After a few hundred megayears, SMBH-B interacts again with the AC-binary, which can be seen from the small SMBH separations and the dip in the AC eccentricity in Figure 2. This interaction ejects SMBH-B to an even wider orbit in the galaxy (Figure 3), from which it takes around a gigayear for it to sink back to the center of the galaxy. Meanwhile, the AC-binary hardens due to stellar scattering, and finally merges due to GW emission ~3 Gyr after the galaxies merged. The remaining AB-binary undergoes a similar evolution, but does not have time to merge before $z = 0$.

The eccentricity of AC shows small oscillations after B enters into a sub ~100 pc hierarchical configuration. Figure 4 shows these oscillations during a period of time when the inner binary has a semimajor axis of $a_{\rm AC} \approx 0.4$ pc, while SMBH-B is on an orbit of $a_{\rm AC-B} \approx 20$ pc with eccentricity $e_{\rm AC-B} \approx 0.79$ at

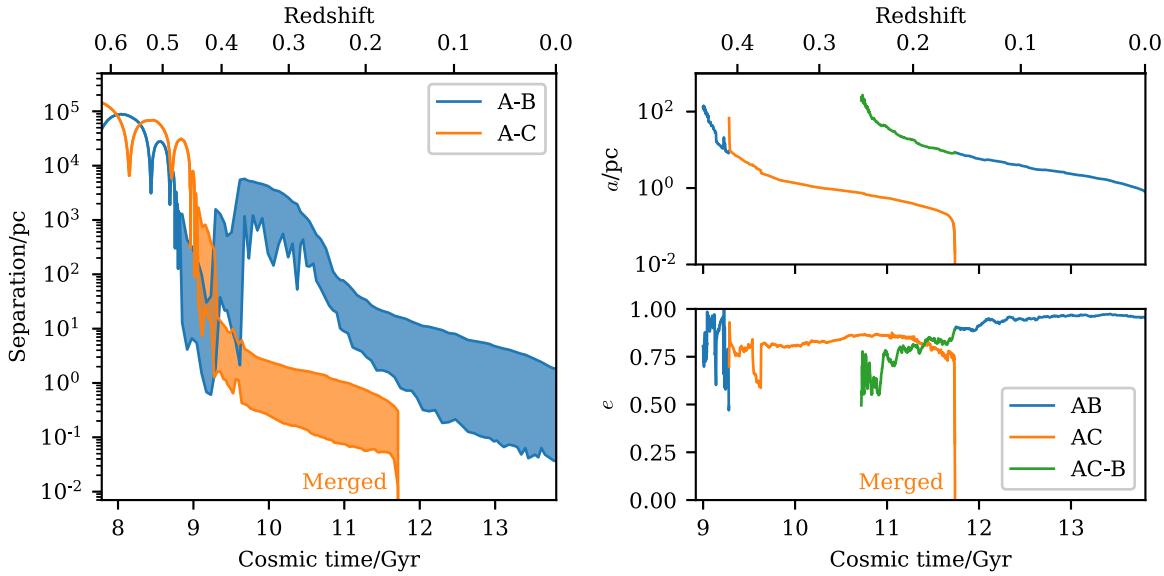

Figure 2. Left: the SMBH A-B and A-C separations over the KETJU simulation. Shaded regions show the range of rapid oscillations. Right: evolution of the semimajor axis a and eccentricity e for the SMBHs in the system. Binaries are labeled by the letters corresponding to their constituent SMBHs (e.g., AB is the binary consisting of SMBHs A and B), while AC-B denotes the orbit of B around the AC-binary in a hierarchical configuration. The remnant of the AC-binary merger is also labeled as A.

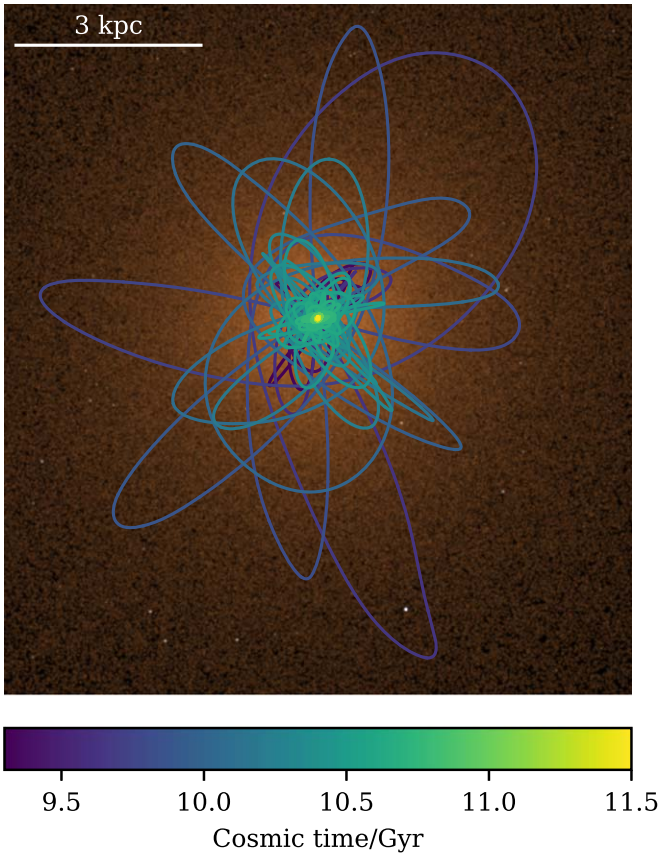

Figure 3. Orbit of the ejected SMBH-B between cosmic times $t = 9.3$ Gyr ($z \sim 0.4$) and $t = 11.5$ Gyr ($z \sim 0.2$) overlaid on the image of the galaxy.

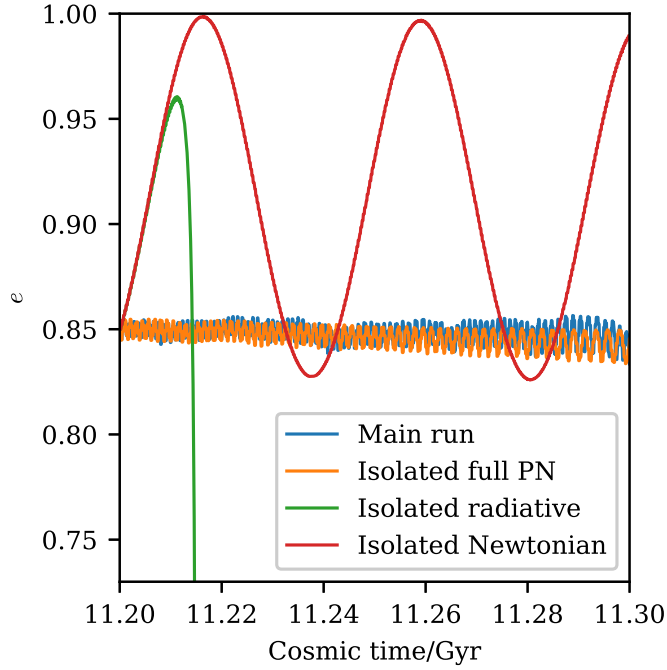

Figure 4. Evolution of the eccentricity e for the inner AC-binary during a part of the phase where the system is in a hierarchical triplet configuration. The evolution is shown for the full cosmological run ("main run") as well as isolated integrations of the triplet starting from the state at cosmic time $t = 11.2$ Gyr using either the full PN equations of motion, including just the leading 2.5PN radiative reaction term or using only Newtonian gravity.

an inclination of $i_{\mathrm{AC-B}} \approx 90°.8$. The oscillations are what remain of Lidov–Kozai oscillations (Lidov 1962) after being suppressed by the relativistic precession of the inner orbit, due to the binary precession period ($\sim 6 \times 10^5$ yr) being much shorter than the Lidov–Kozai oscillation period ($\sim 4 \times 10^7$ yr) (Holman et al. 1997; Blaes et al. 2002; Bonetti et al. 2016). A comparison to an isolated integration of the system using only Newtonian gravity shows that the system would indeed undergo large eccentricity oscillations without the inclusion of relativistic precession from the 1PN level corrections. With the addition of only the gravitational radiation reaction terms the inner binary would merge rapidly due to these oscillations, which serves to illustrate that the added complexity of the other PN correction terms is necessary for correctly handling BH triplets or even more complex systems.

Our KETJU PN correction implementation includes only PN terms relevant for binaries, ignoring three-body cross terms appearing at 1PN level (e.g., Thorne & Hartle 1985). It has been argued that these terms can in some cases lead to significant effects over long enough time periods (Will 2014; Lim & Rodriguez 2020). However, in this specific case the ignored terms do not appear to lead to significant changes in the behavior of the system. This is demonstrated by an isolated integration of the SMBH triplet using a version of the integrator including also the 1PN level three-body terms, shown in Figure 4. The results are visually almost indistinguishable from the main run, and utilizing additional integrations without the three-body terms we have confirmed that the small differences between the runs are due to stellar interactions. However, in some other triplet configurations the cross terms may result in more significant effects, and thus including them in future simulations seems prudent.

3.3. SMBH Binary Hardening Rate

To confirm that the SMBH binary hardening process is modeled correctly in a cosmological simulation, when including also stellar softening in the regularized regions, we fit the binary hardening rate using the Quinlan (1996) model

$$\frac{da^{-1}}{dt} = (aK)^{-1}\frac{de}{dt} = H\frac{G\rho}{\sigma}, \quad (1)$$

where the stellar density ρ and velocity dispersion σ are computed within the influence radius $R_{\rm inf} \approx 500$ pc of the binary and K and H are constants. Performing the fit when the binary semimajor is around $a \sim 2$ pc, we get for the AC-binary at cosmic time $t \approx 10.4$ Gyr the values $H \approx 12$, $K \approx 0.1$, and for the AB-binary at $t \approx 12.4$ Gyr the slightly lower values $H \approx 5.2$, $K \approx 0.02$. These results are comparable to the values obtained for our isolated elliptical galaxy merger simulations (Mannerkoski et al. 2019). Based on these fits and using also analytical expressions for the effects of GW emission (Peters 1964), we find that the AB-binary would merge within ~ 400 Myr after the end of the simulation.

3.4. Effects on the Stellar Density

With KETJU it is also possible to capture the effects of SMBH binaries on the stellar distribution of the galaxies. The evolution of the central stellar density around SMBH-A is shown in Figure 5. The GADGET-3 run shows only a very gradual decrease after the galaxy mergers have occurred and the SMBHs have merged at a separation of around one softening length. In contrast, the KETJU run shows a rapid ejection of stars after the formation of the bound SMBH system, tapering off to a more gradual decrease similar to the GADGET-3 run after ~ 1 Gyr. The final stellar density of the KETJU run is lower by $\sim$30%, although the effect of the SMBH binaries on the stellar density in the KETJU run is not quite as prominent as in some of our earlier isolated merger studies (Rantala et al. 2018), due to the lower masses of the SMBHs in the present study.

4. Conclusions

We have shown here how KETJU can be applied to cosmological zoom simulations to capture the dynamics of massive SMBHs including also the complex behavior of SMBH triplets. Our simulations are also able to resolve the effect of SMBH binaries on the distribution of stars in the central regions of the host galaxy, which can then affect the hardening rate and merger timescale of subsequently formed SMBH binaries in the same galaxy. Modeling multiple SMBH systems and the detailed SMBH binary stellar interactions using only simple orbit-averaged semianalytic models is currently not feasible. The methods applied here can also be extended to study larger systems hosting tens of massive SMBHs, with the main challenges including the relatively high required stellar mass resolution and the high computational cost of the regularized integration.

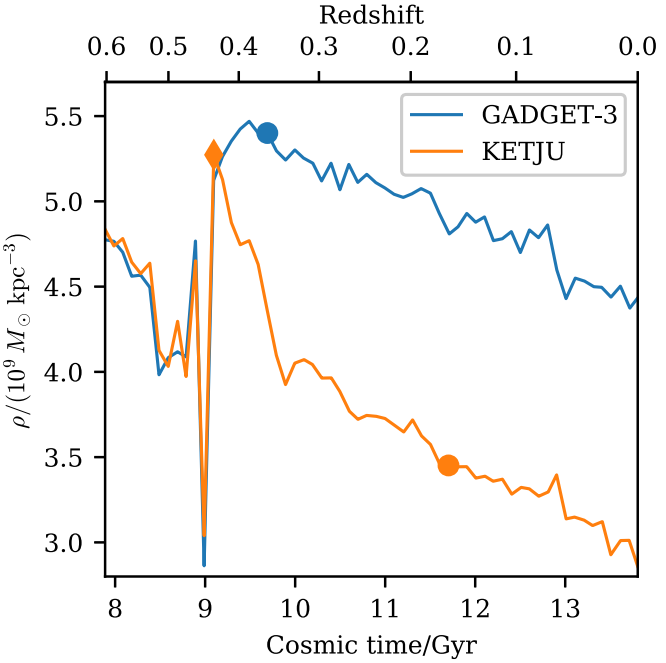

Figure 5. Evolution of the mean stellar density ρ within a $r = 500$ pc sphere at the center of galaxy A. The size of the sphere is approximately the same as the sphere of influence of the SMBH. The circles mark SMBH mergers, and the diamond indicates when a bound binary was first formed in the KETJU run.

The triple galaxy merger and the ensuing SMBH interactions presented here demonstrate some key dynamical processes that complicate the SMBH merger process in such systems compared to simple binary systems. First, strong three-body interactions resulted in the ejection of one SMBH to a wide orbit where it spent several gigayears. In a system, which is sufficiently gas-rich, such an ejected SMBH could potentially be observable as an offset AGN long after the initial galaxy mergers. At a later stage the SMBH triplet entered a hierarchical configuration, but due to relativistic precession there were no significant effects on orbit or the merger timescale of the inner binary. Had the inner binary been on a wider orbit with slower precession, the eccentricity oscillations caused by the Lidov–Kozai mechanism could have significantly sped up the merger, as was the case in the comparison integration with the precession effects disabled. Detailed modeling of SMBHs in their global environment is therefore a crucial tool for understanding the evolution and final fate of systems hosting multiple SMBHs.

M.M., P.H.J., and S.L. acknowledge the support by the European Research Council via ERC Consolidator Grant KETJU (No. 818930).

T.N. acknowledges support from the Deutsche Forschungsgemeinschaft (DFG, German Research Foundation) under

Germany's Excellence Strategy—EXC-2094-390783311 from the DFG Cluster of Excellence "ORIGINS."

The numerical simulations used computational resources provided by the CSC—IT Center for Science, Finland.

Software: KETJU (Rantala et al. 2017, 2020), GADGET-3 (Springel 2005), NumPy (Harris et al. 2020), SciPy (Virtanen et al. 2020), Matplotlib (Hunter 2007), pygad (Röttgers et al. 2020), MUSIC (Hahn & Abel 2011, 2013).

ORCID iDs

Matias Mannerkoski https://orcid.org/0000-0001-5721-9335
Peter H. Johansson https://orcid.org/0000-0001-8741-8263
Antti Rantala https://orcid.org/0000-0001-8789-2571
Thorsten Naab https://orcid.org/0000-0002-7314-2558
Shihong Liao https://orcid.org/0000-0001-7075-6098

References

Aumer, M., White, S. D. M., Naab, T., & Scannapieco, C. 2013, MNRAS, 434, 3142
Begelman, M. C., Blandford, R. D., & Rees, M. J. 1980, Natur, 287, 307
Blaes, O., Lee, M. H., & Socrates, A. 2002, ApJ, 578, 775
Bonetti, M., Haardt, F., Sesana, A., & Barausse, E. 2016, MNRAS, 461, 4419
Bonetti, M., Sesana, A., Haardt, F., Barausse, E., & Colpi, M. 2019, MNRAS, 486, 4044
Chandrasekhar, S. 1943, ApJ, 97, 255
Deane, R. P., Paragi, Z., Jarvis, M. J., et al. 2014, Natur, 511, 57
Eisenreich, M., Naab, T., Choi, E., Ostriker, J. P., & Emsellem, E. 2017, MNRAS, 468, 751
Hahn, O., & Abel, T. 2011, MNRAS, 415, 2101
Hahn, O., & Abel, T. 2013, MUSIC: MUlti-Scale Initial Conditions, Astrophysics Source Code Library, ascl:1311.011
Harris, C. R., Millman, K. J., van der Walt, S. J., et al. 2020, Natur, 585, 357
Hills, J. G., & Fullerton, L. W. 1980, AJ, 85, 1281
Hoffman, L., & Loeb, A. 2007, MNRAS, 377, 957
Holman, M., Touma, J., & Tremaine, S. 1997, Natur, 386, 254
Hu, C.-Y., Naab, T., Walch, S., Moster, B. P., & Oser, L. 2014, MNRAS, 443, 1173
Hunter, J. D. 2007, CSE, 9, 90
Johansson, P. H., Burkert, A., & Naab, T. 2009a, ApJL, 707, L184
Johansson, P. H., Naab, T., & Burkert, A. 2009b, ApJ, 690, 802
Kelley, L. Z., Blecha, L., & Hernquist, L. 2017a, MNRAS, 464, 3131
Kelley, L. Z., Blecha, L., Hernquist, L., Sesana, A., & Taylor, S. R. 2017b, MNRAS, 471, 4508
Khan, F. M., Fiacconi, D., Mayer, L., Berczik, P., & Just, A. 2016, ApJ, 828, 73
Kollatschny, W., Weilbacher, P. M., Ochmann, M. W., et al. 2020, A&A, 633, A79
Kormendy, J., & Ho, L. C. 2013, ARA&A, 51, 511
Lidov, M. L. 1962, P&SS, 9, 719
Lim, H., & Rodriguez, C. L. 2020, PhRvD, 102, 064033
Liu, X., Hou, M., Li, Z., et al. 2019, ApJ, 887, 90
Mannerkoski, M., Johansson, P. H., Pihajoki, P., Rantala, A., & Naab, T. 2019, ApJ, 887, 35
Mikkola, S., & Merritt, D. 2008, AJ, 135, 2398
Mora, T., & Will, C. M. 2004, PhRvD, 69, 104021
Peters, P. C. 1964, PhRv, 136, 1224
Peters, P. C., & Mathews, J. 1963, PhRv, 131, 435
Pfeifle, R. W., Satyapal, S., Manzano-King, C., et al. 2019, ApJ, 883, 167
Pfister, H., Volonteri, M., Dubois, Y., Dotti, M., & Colpi, M. 2019, MNRAS, 486, 101
Planck Collaboration, Aghanim, N., Akrami, Y., et al. 2020, A&A, 641, A6
Quinlan, G. D. 1996, NewA, 1, 35
Rantala, A., Johansson, P. H., Naab, T., Thomas, J., & Frigo, M. 2018, ApJ, 864, 113
Rantala, A., Johansson, P. H., Naab, T., Thomas, J., & Frigo, M. 2019, ApJL, 872, L17
Rantala, A., Pihajoki, P., Johansson, P. H., et al. 2017, ApJ, 840, 53
Rantala, A., Pihajoki, P., Mannerkoski, M., Johansson, P. H., & Naab, T. 2020, MNRAS, 492, 4131
Röttgers, B., Naab, T., Cernetic, M., et al. 2020, MNRAS, 496, 152
Ryu, T., Perna, R., Haiman, Z., Ostriker, J. P., & Stone, N. C. 2018, MNRAS, 473, 3410
Scannapieco, C., Tissera, P. B., White, S. D. M., & Springel, V. 2005, MNRAS, 364, 552
Scannapieco, C., Tissera, P. B., White, S. D. M., & Springel, V. 2006, MNRAS, 371, 1125
Sijacki, D., Springel, V., Di Matteo, T., & Hernquist, L. 2007, MNRAS, 380, 877
Springel, V. 2005, MNRAS, 364, 1105
Springel, V., Di Matteo, T., & Hernquist, L. 2005, MNRAS, 361, 776
Thorne, K. S., & Hartle, J. B. 1985, PhRvD, 31, 1815
Tremmel, M., Governato, F., Volonteri, M., & Quinn, T. R. 2015, MNRAS, 451, 1868
Virtanen, P., Gommers, R., Oliphant, T. E., et al. 2020, NatMe, 17, 261
Will, C. M. 2014, PhRvD, 89, 044043